PERIODICO di MINERALOGIA
established in 1930

DIPARTIMENTO
DI SCIENZE DELLA TERRA
SAPIENZA
UNIVERSITÀ DI ROMA

An International Journal of
Mineralogy, Crystallography, Geochemistry,
Ore Deposits, Petrology, Volcanology
and applied topics on Environment, Archaeometry and Cultural Heritage

Origin of graphic texture by magma mixing-induced undercooling in the Borjuri diorite pluton, Mikir Massif, Northeast India

Tribujjal Prakash, Pallabi Basumatary, Bibhuti Gogoi *

Department of Geology, Cotton University, Guwahati, Assam 781001, India

ARTICLE INFO

Submitted: June 2024
Accepted: November 2024
Available on line: November 2024

* Corresponding author:
bibhuti.gogoi.baruah@gmail.com

Doi: 10.13133/2239-1002/18561

How to cite this article:
Prakash T. et al. (2024)
Period. Mineral. 93, 201-220

ABSTRACT

Graphic intergrowths from the Borjuri diorite pluton in the Mikir Massif of Northeast India were investigated to reflect on the role of magma mixing in their formation. The work presented discusses how magma mixing triggers an abrupt change in liquidus temperature (undercooling), driving the formation of graphic intergrowths. Previously, fractal dimensions were utilised in experimental work to understand the involvement of undercooling in graphic texture formation. The present study follows the earlier documented experimental work and puts forward a new approach, as it employs fractal and lacunarity calculations in natural systems (i.e., natural diorite from the Mikir Massif). The fractal and lacunarity calculations presented in this work demonstrate the complexity of graphic intergrowths, in order to qualitatively assess the relative degree of undercooling. Undercooling, resulting from the rise in liquidus temperature, was achieved due to loss of volatiles or devolatilization during magma mixing. Observed disequilibrium textures such as rapakivi, anti-rapakivi, skeletal amphiboles, acicular apatite, biotite clots, dendritic and zoned plagioclase, provides a reliable explanation for an origin linked to magma mixing, further providing a different perspective for the growth of such graphic intergrowths. Signatures of magma mixing have been reported from numerous Pan-African felsic plutons in the Assam-Meghalaya Gneissic Complex. Considering the regional viewpoint and the textural signatures observed in the diorites, magma mixing could be the only plausible explanation for the formation of the diorites.

Keywords: graphic texture; fractal analysis; box-counting; lacunarity; rapakivi; anti-rapakivi.

INTRODUCTION

Igneous rocks are noteworthy for their display of a variety of textures (Lee, 1997). Textural studies can be pivotal in unravelling the behaviour of magmatic systems and magma chamber dynamics. Texture formation is mainly governed by two processes- crystal nucleation and crystal growth (Swanson, 1977; Rusiecka and Baker, 2021). Graphic texture comprises of cuneiform quartz crystals, which results from skeletal growth of hexagonal quartz within host K-feldspar. This heterogeneous texture, commonly found in granitic bodies, is associated with rapid crystal growth, and is considered to form as a consequence of non-equilibrium crystallizing conditions (Barker 1970; Rusiecka and Baker, 2021). With regard to the formation of graphic texture, quite a few hypotheses have been proposed. Originally it was put forward that simultaneous growth of quartz and feldspar near the thermal minimum was the main process behind the formation of the texture (Barker, 1970; Hughes, 1971). However, Smith (1974), Walker (1976), Fenn (1986), and London et al. (1989) suggested that the texture may not form under equilibrium conditions but near cotectic or eutectic of the system. Fenn (1986) further focused on the role of growth kinetics and diffusion through experimental

work on a granite bulk composition. Rapid crystallization under volatile saturated conditions is also considered to be a reason for the formation of graphic and granophyric textures (Barker, 1970; Hibbard, 1980; Martin, 1982).

Textural variations in igneous rocks are function of the phases involved, chemical compositions of the phases, the melt associated with it, pre-existing phase boundaries, deformation post phase crystallization, and degree of undercooling (Candela, 1997). The degree of undercooling for a given phase influences the crystal morphology and kinetics in a crystallizing system (Swanson, 1977). Undercooling (ΔT) serves as the driving factor for crystal nucleation and growth and is defined as the difference between the temperatures of melt saturation with respect to a mineral (MacLellan and Trembath, 1991). A melt may crystallize and give rise to a coarse-grained texture at low undercooling, whereas with increasing undercooling, crystallization textures evolve into a finer variety (Vernon, 1990; Candela, 1997). The phenomenon of undercooling requires an instant cooling mechanism. For instance, ascent of undersaturated magma into country rocks at shallower level maximizes the thermal difference between the magma and the country rocks. Moreover, undercooling is also crucial for the nucleation of crystals and their growths and hence increasing undercooling controls the evolution of crystallization textures (Stemprok et al., 2008). Therefore, granophyre, skeletal quartz, quartz-dendrites, and graphic textures must undergo a suitable degree of undercooling for their initiation (Candela, 1997).

The concept of fractal was framed around the principle of scale invariance or self-similarity (Mandelbrot, 1967). Fractal dimension deals with describing the complexity of a pattern or geometry. For example, a line (one-dimensional) has a fractal dimension of 1, whereas a plane (two-dimensional) has a fractal dimension of 2. If a pattern has a fractal dimension of 1.4, it indicates that the pattern is more complex than a line but less complex compared to a plane. Thus, calculation of fractal dimension allows examining and differentiating the intricacy of various fractal patterns (Fowler, 1995). The incorporation of fractal methods in geosciences has slowly developed an interest in the use of fractal calculations in geological patterns (Hu et al., 2018). Although there are a few applications of fractal calculation in petrology, fractal geometry remains a potent tool for measuring intricate patterns in rocks (Perugini et al., 2003; Slaby et al., 2012; Hu et al., 2018; Rusiecka and Baker, 2021). This method has therefore been handy in understanding textural parameters, distribution of minerals, and their morphology (Fowler, 1995). Fractal analyses, which accurately and repetitively delineates the crystal boundary, facilitates comparison of results, and illustrates the distinction between different minerals (Huber and Stępniewska, 2021). The advantage of fractal analyses in geology is evident in its ability to quantify, often with a single parameter (fractal dimension, D_{box}), complex processes that would otherwise be challenging to assess using conventional geological methods (Hu et al., 2018). Mandelbrot (1982) and Fowler (1995) put forward a method where the pattern complexity of an image is calculated (box-counting). Rusiecka and Baker (2021) observed and calculated the textural evolution of graphic intergrowths using fractal analyses. They also stressed upon the possibility of using fractal mechanisms to quantify graphic intergrowths to indicate the deviation from equilibrium, given that the degree of undercooling is linked with the parameters (box-counting and lacunarity) obtained through fractal measurements. Perugini et al. (2003) used the box-counting technique to analyze the structures resulting from magma mixing processes. Moreover, Hu et al. (2018) also used fractal analyses to observe the amphibole aggregation growth from a basaltic melt.

In this paper, we shed light on the role of magma mixing in the formation of quartz graphic intergrowths. Our investigations are primarily conducted through petrographic studies and have been further advanced by implementing fractal and lacunarity calculations on natural graphic textures. While fractal dimension and lacunarity calculations have previously been used to understand the evolution of graphic texture, these analyses were limited to experimental samples (Rusiecka and Baker, 2021). In the present study, we have built upon their experimental work and adapted it to natural rock samples, examining the graphic intergrowths to comment on the influence of undercooling for their generation. The complexity of the quartz graphic intergrowths is measured by the box-counting fractal dimension, while lacunarity measures how the texture fills the space between them. Focusing on the varied morphologies, this approach provides new interpretations of the varying degrees of undercooling, potentially arising from devolatilization driven by magma mixing. This distinction sets our work apart from earlier studies and offers additional insights into the textural evolution within natural systems.

GEOLOGICAL SETTING AND FIELD RELATIONS

The framework of Assam-Meghalaya Gneissic Complex (AMGC) may be defined as an uplifted horst-like structure which encompasses two Precambrian crustal blocks, viz., Shillong Plateau and Mikir Massif of Northeast India. These blocks are detached by the NW-SE trending Kopili lineament. The AMGC comprises rocks of Archean to Late Proterozoic, Cambrian, Permian, Triassic, Cretaceous, Tertiary, and Quaternary periods (Nandy, 2001; Srivastava and Sinha, 2004). The AMGC is the exclusive depiction of Precambrian rocks in Northeast

India, and is also regarded as a part of the eastward extension of the Central Indian Tectonic Zone (Figure 1; Gogoi, 2022). It has been cut off from the mainland India by the Garo-Rajmahal depression. The geology of Shillong Basin, which occupies central and eastern part of Meghalaya plateau and northwestern part of Mikir Massif, dates back to early Proterozoic, when rifting was initiated by the process of back-arc spreading (Basumatary et al., 2023). Sedimentation within this rift basin resulted in the formation of Shillong Group of rocks (Bhattacharjee and Rahman, 1985). The Shillong Group of metasedimentary rocks were later intruded by younger felsic and mafic magmas episodically.

The present study area is located within the periphery of Shillong Basin part of Mikir Massif, which lies in the easternmost domain of AMGC. Lithologically, the Mikir Massif consists of sillimanite-bearing gneisses, metadolerites, granulites, banded iron formation, and granite gneisses (Ghosh et al., 2005; Gogoi et al., 2019; Basumatary et al., 2023). However, the Shillong Group of rocks within Mikir Massif are exemplified by quartzites, cross-bedded arenites, conglomerates, volcanoclastics, and various low-grade schists like garnetiferous, ferruginous, and quartz sericite schists (Dhurandhar et al., 2019). Several magmatic events resulted in the intrusion of numerous felsic, intermediate, and mafic rocks within the basement gneisses and metasediments of Shillong Group. The Kathalguri, Bamuni, and Kaziranga granite plutons along with the Borjuri diorite pluton, serve as examples of Pan-African magmatism in the region (Majumdar and Dutta, 2016; Kumar et al., 2017; Hazarika and Gogoi, 2023; Hazarika et al., in preparation; Prakash et al., 2023). Moreover, Hayajuri and Borjuri Proterozoic metadolerites (Khasi greenstones) are also found as intrusives within basement gneissic complex and Shillong Group of metasedimentary rocks (Dhurandhar et al., 2019; Basumatary et al., 2023).

The present study was conducted on the diorite pluton of Borjuri area in the Mikir Massif (Figure 2). This dioritic pluton is found in contact with the metadolerites and quartzites of the Shillong Group. The studied diorites are coarse-grained and mesocratic in nature and shows no

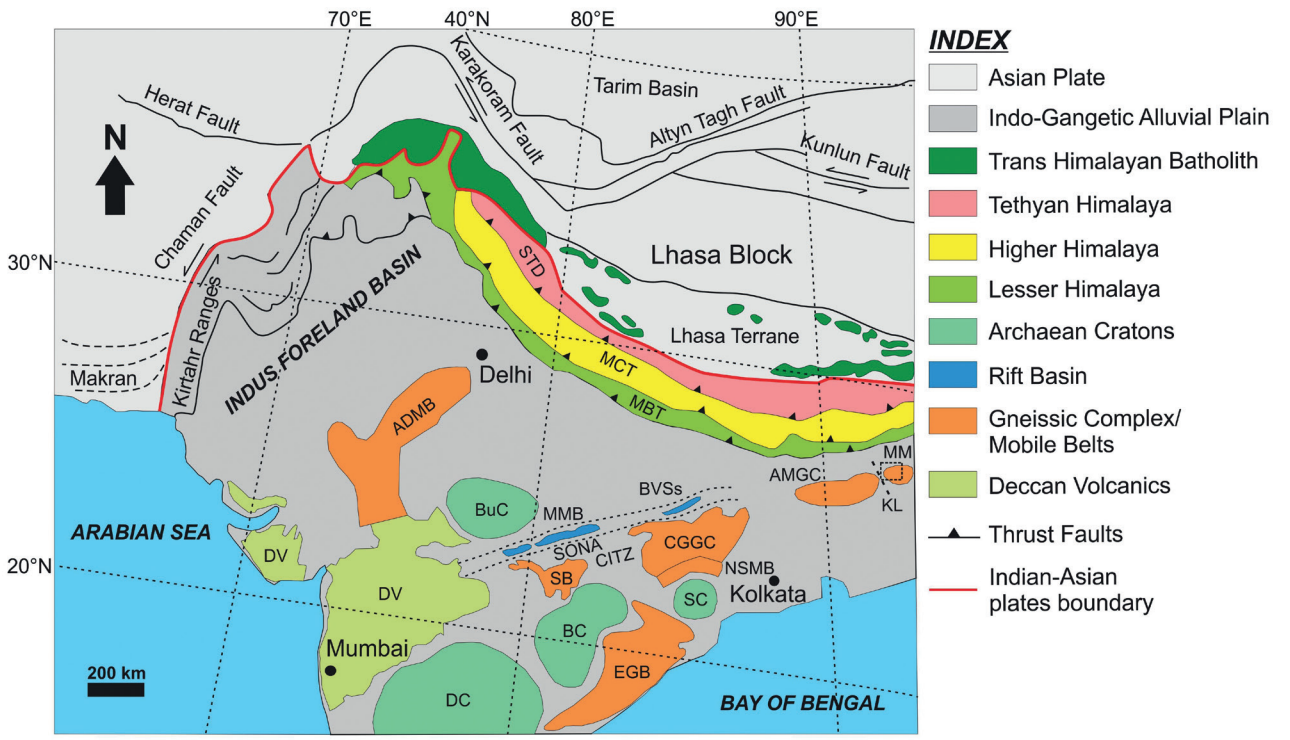

Figure 1. Geological and tectonic map of India and its surrounding region showing the location of Mikir Massif (MM) with respect to Archaean cratons and Proterozoic mobile belts (modified after Borah et al., 2023). The MM is marked by black dashed box. Abbreviations: ADMB = Aravalli Delhi Mobile Belt, BC = Bastar Craton, BuC = Bundelkhand Craton, BVSs = Bathani volcano-sedimentary sequence, CGGC = Chotanagpur Granite Gneiss Complex, CITZ = Central India Tectonic Zone, DC = Dharwar Craton, DV = Deccan Volcanics, EGB = Eastern Ghats Belt, KL = Kopili Lineament, MBT = Main Boundary Thrust, MCT = Main Central Thrust, MMB = Mahakoshal Mobile Belt, NSMB = North Singhbhum Mobile Belt, SB = Satpura Belt, SC = Singhbhum Craton, SONA = Son-Narmada graben, STD = South Tibetan Detachment.

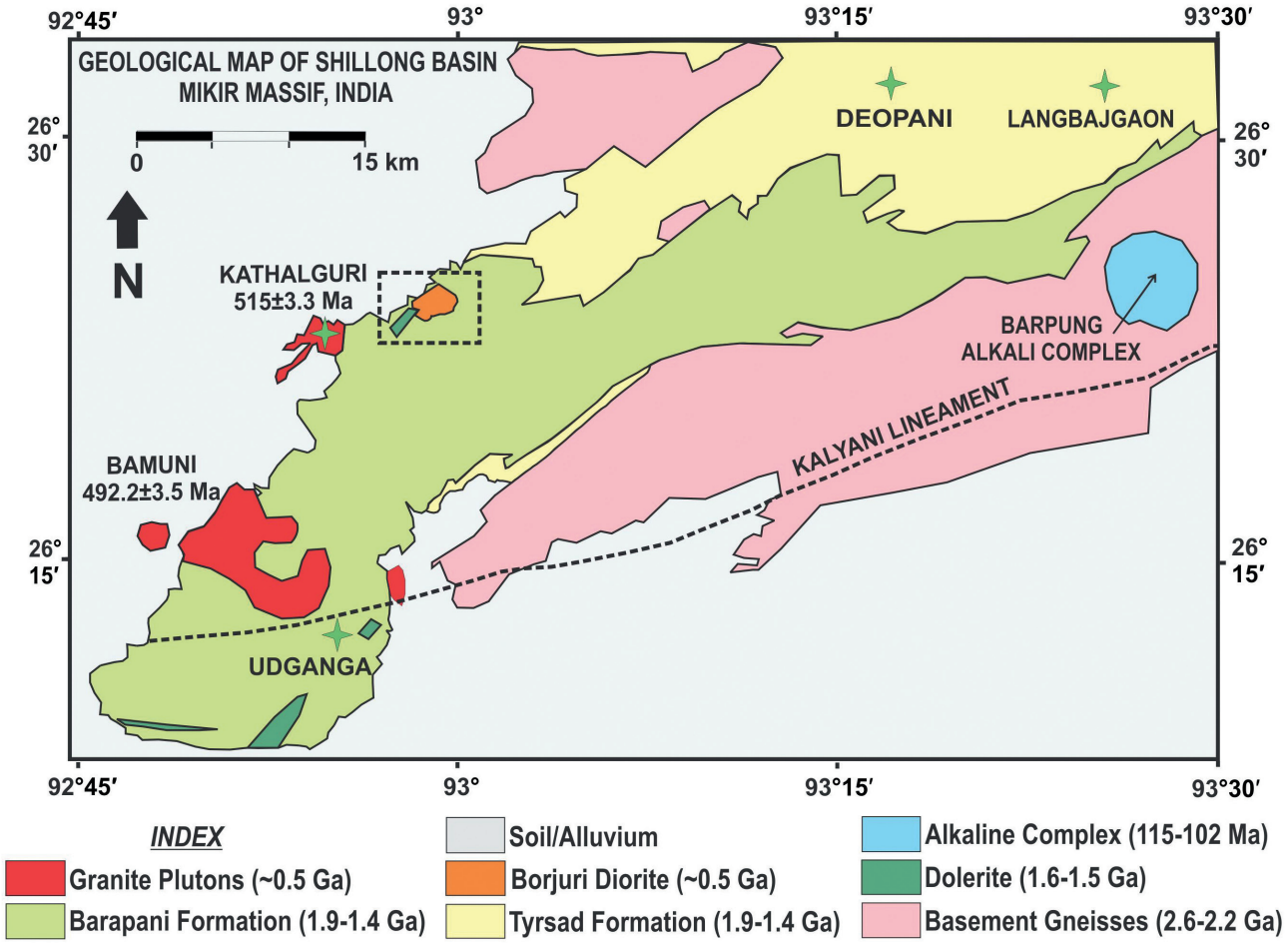

Figure 2. Simplified regional geological map of the Mikir Massif, Northeast India showing the study area (Borjuri Pluton) within the black box (modified after Dhurandhar et al., 2019).

sign of metamorphism (Figure 3 a,b). Exfoliation or onion skin weathering can also be noticed in the outcrop (Figure 3c). Moreover, K-feldspars, distinguished by their pink colour, are prominently visible in the rocks (Figure 3d). Determining the exact area covered by the diorite pluton is challenging due to thick vegetation cover, which obscures much of its visibility. It is also considered that the Borjuri diorites were emplaced in a post-collisional extension regime as a result of Pan-African post-collisional rift-induced magmatism (Prakash et al., 2023).

ANALYTICAL METHODS

The majority of the studied diorite pluton in the Borjuri area is mainly obscured by vegetation. However, the north-eastern part of the pluton is quarried and hence fresh samples were collected from the quarry. Thin section preparation was carried out from the collected samples for petrographic study. A total of 10 slides were prepared for petrographic study and mineral chemical analyses. Petrographic studies were carried out using the Leica DM 2700P microscope in the Igneous Petrology Laboratory, Department of Geology, Cotton University, Assam. Mineral chemical analyses were carried out with the help of a CAMECA SX-Five electronprobe microanalyzer (EPMA) at the Department of Earth Sciences, Indian Institute of Technology, Bombay. The analytical conditions were: 15 kV accelerating voltage, 20 nA beam current, and 1 μm beam diameter. Mineral standards used to calibrate major elements were albite (Si K_a, Na K_a), Al_2O_3 (Al K_a), diopside (Mg K_a), Fe_2O_3 (Fe K_a), K-feldspar (K K_a), rhodonite (Mn K_a), TiO_2(Ti K_a), Cr_2O_3(Cr K_a), ZnS (Zn K_a), $BaSO_4$(Ba L_a), NaCl (Cl K_a), and apatite (Ca K_a, F K_a).

Rusiecka and Baker (2021) used fractal calculations to comment on the influence of varying degree of undercooling on the evolution of experimentally derived graphic intergrowths. Following their method, we have qualitatively tried to assess the changing degree of

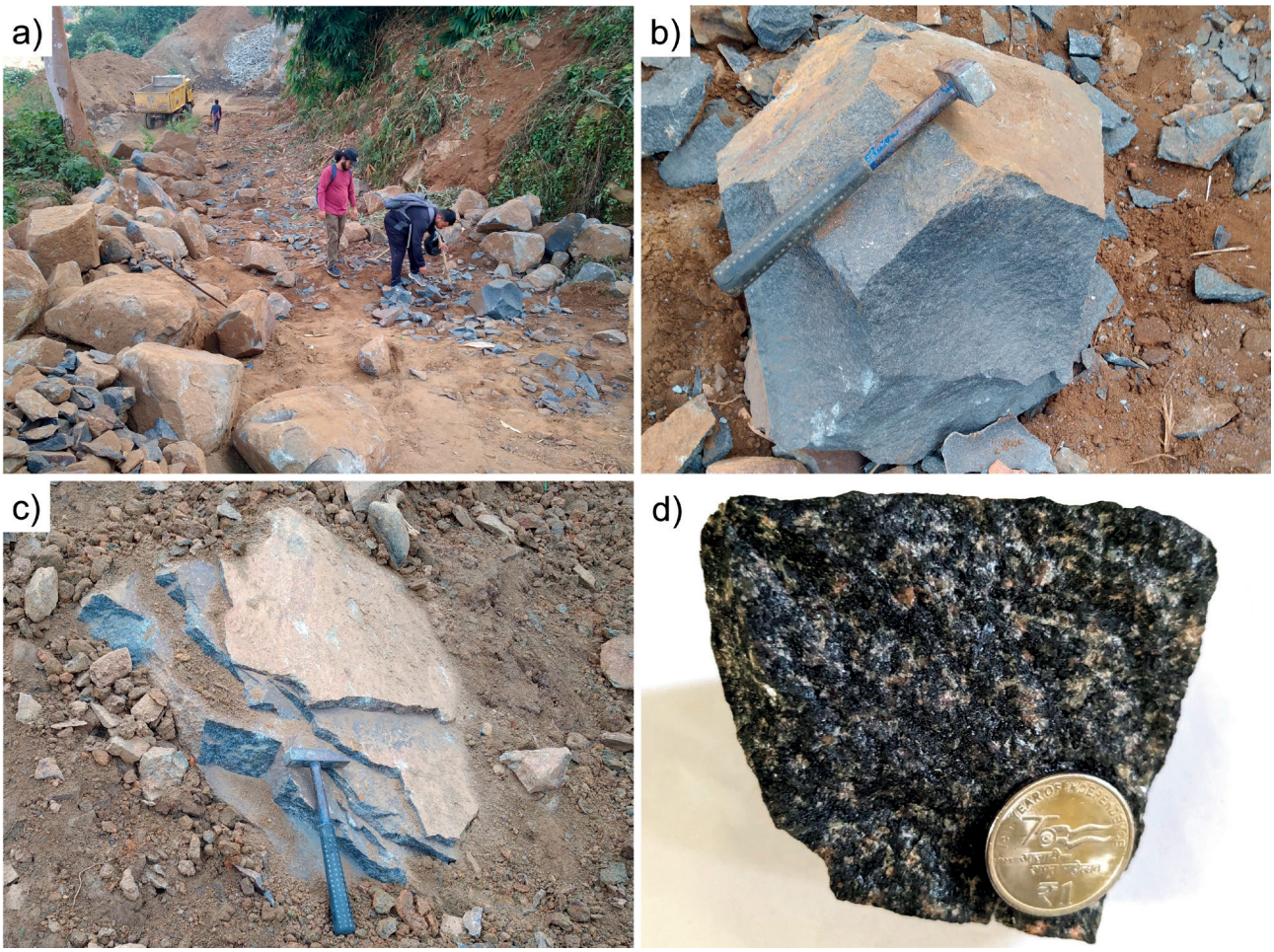

Figure 3. Photographs showing the field relationships of the Borjuri diorite pluton. a-c) Diorite pluton exposures. d) Hand sample of the diorite with distinct pink K-feldspar.

undercooling from natural quartz graphic intergrowths using box-counting fractal dimensions, (D_B) and lacunarity calculations, (Λ). The image is placed with grids of different dimensions and the number of grids covering a certain object is measured. Lacunarity, in addition, provides us the measure of how a pattern bridges the gaps. Therefore, an image with more gaps in between patterns will show higher lacunarity as opposed to patterns which have lesser space (Rusiecka and Baker, 2021). The box-counting fractal dimensions, D_B (Fowler, 1995, Smith et al., 1996) and the lacunarity calculations, Λ (Mandelbrot, 1982, Smith et al., 1996) were calculated in binary images from the FracLac plugin in ImageJ software (Karperien, 1999-2013). In this study, fractal and lacunarity calculations of quartz graphic intergrowths were made from selected images. The best images of graphic texture with quartz grains showing variation in morphologies were chosen. The images were cropped so as to only incorporate the graphic intergrowths for calculations. The images were converted into greyscale using CorelDRAW graphic editor and subsequently converted to binary images for calculations. The white elements considered in the image are the quartz crystals whereas the black background is K-feldspar.

RESULTS

Petrography

Petrographic descriptions of the Borjuri diorites have been reported earlier (Prakash et al., 2023). A brief account of the petrography along with new observations are summarised here. The diorites have an inequigranular mineralogical assemblage dominated by quartz, K-feldspar, plagioclase, biotite, and amphibole with minor proportions of titanite, calcite, epidote, apatite, zircon, and iron oxides. The mineral grains range from euhedral to anhedral in shape. Plagioclase occurs as the predominant phenocryst phase with variation in grain size. They are distributed as lath-shaped grains (0.04-

0.10 mm) and stout rectangular phenocrysts (0.31-0.72 mm) throughout the samples. The smaller lath-shaped crystals tend to be more euhedral, whereas the larger grains are subhedral to anhedral in nature. A significant fraction of the plagioclase phenocrysts have experienced different degrees of resorption (Figure S1 a,b). Most of these resorbed plagioclase crystals have ragged, sieve-textured occurrence (Figure S1 b-e). Quartz commonly occurs as inequigranular irregular grains in association with K-feldspar and even as individual anhedral masses. Amphiboles can be divided into three textural types: small, green, needle-like grains of approximately 0.005 mm in width; larger, green, subhedral to euhedral prismatic skeletal grains (0.41-0.62 mm) (Figure 4a); and medium to large, brownish, ragged anhedral masses (0.07-0.15 mm). Biotite crystals appear as brown laths; they are either present as isolated grains or occur interstitially between phenocrysts as clots (Figure 4b). Apatites present in the rock are needle-like, acicular in nature (Figure 4 c,d). K-feldspar primarily serves as the host material upon which quartz nucleates to create graphic texture. K-feldspar also forms outer rims around plagioclase crystals depicting anti-rapakivi texture (Figure 5 a,b; Figure S1f). Moreover, plagioclase has been observed surrounding resorbed K-feldspar crystals representing rapakivi texture (Figure 5 c,d; Figure S2).

The diorites are characterised by holocrystalline, allotriomorphic texture and also reveal some special types of disequilibrium textures, such as, 1) rapakivi texture, 2) anti-rapakivi texture, 3) non-dendritic plagioclase with a dendritic plagioclase mantle, 4) zoned plagioclase crystals, 5) biotite clots, 6) skeletal amphibole, 7) acicular apatite, 8) graphic texture, and 9) graphic texture mantle on plagioclase. Rapakivi texture is characterized by resorbed

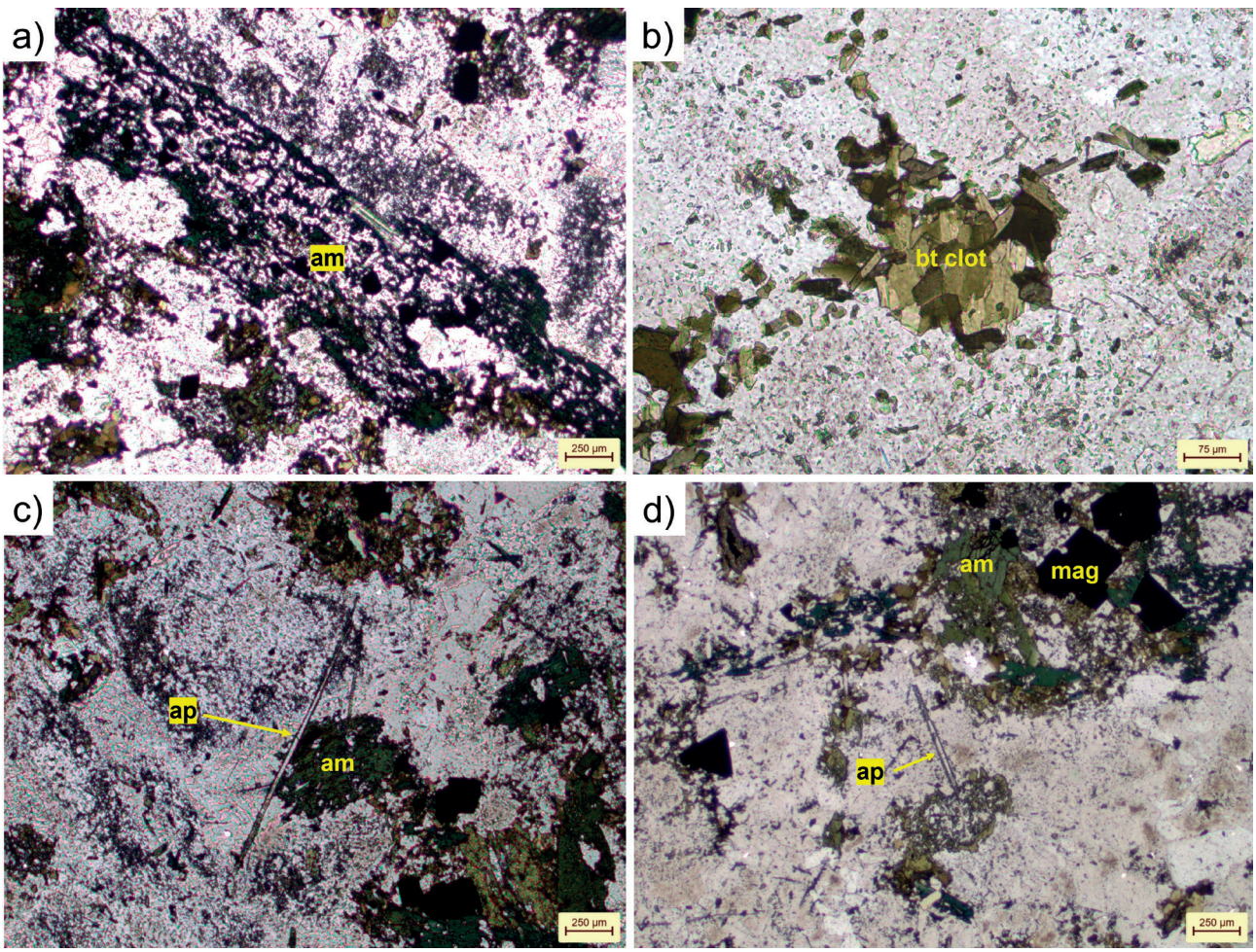

Figure 4. Transmitted light photomicrographs of the studied samples. Parallel polars. a) Prismatic skeletal amphibole. b) Cluster of small biotites forming clot. c) Needle-like acicular apatite with amphiboles of ragged nature. d) Assemblage of acicular apatite, amphibole and magnetite. Abbreviations: am = amphibole, ap = apatite, bt = biotite, mag = magnetite.

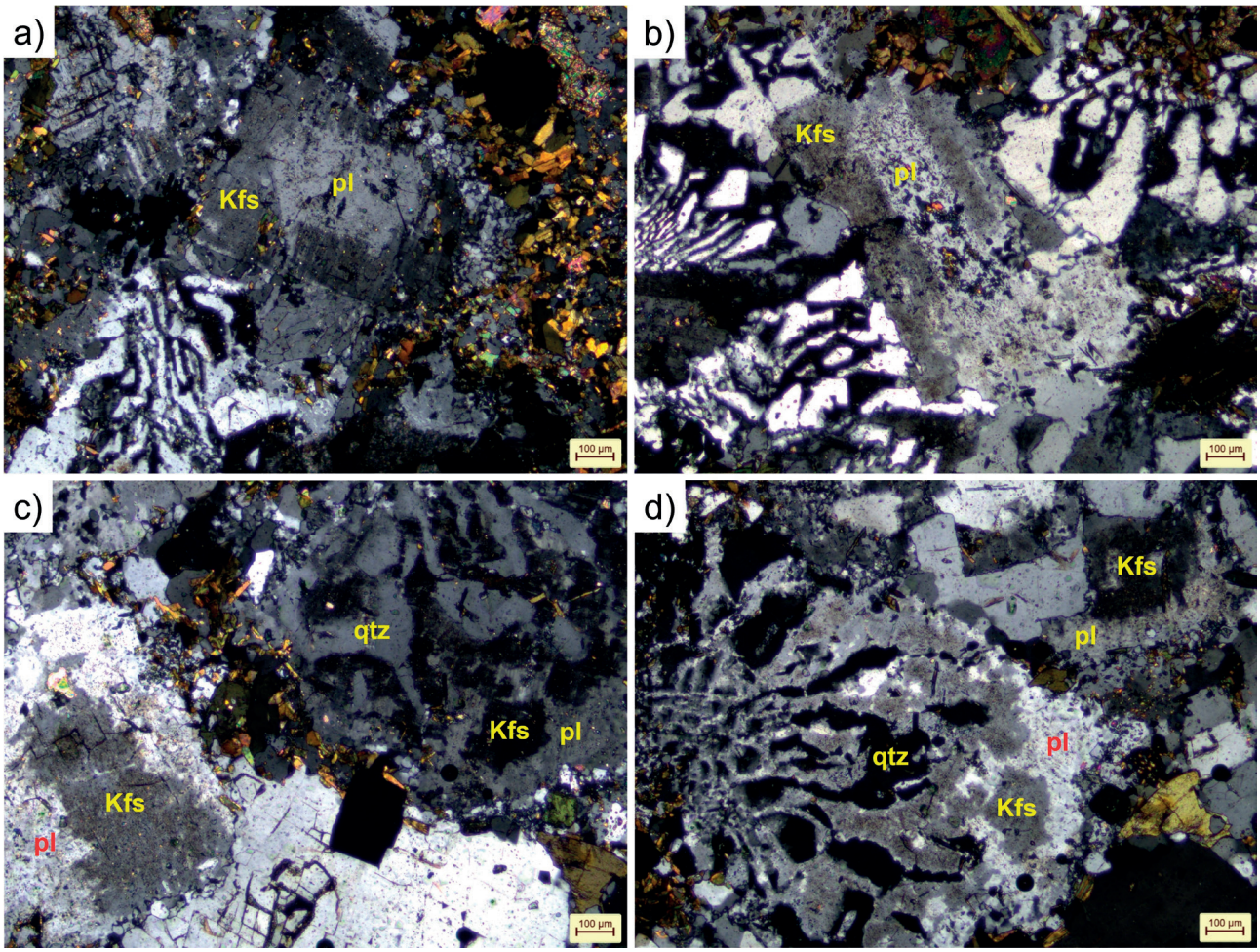

Figure 5. Detailed photomicrographs of the studied samples. Crossed polars, transmitted light. a,b) Resorbed plagioclase with outer rim of K-feldspar demonstrating anti-rapakivi texture with adjacent quartz-feldspar intergrowths. c,d) Quartz-feldspar intergrowth mantled by plagioclase and plagioclase mantled on resorbed grains of K-feldspar signifying rapakivi texture. Abbreviations: Kfs = K-feldspar, pl = plagioclase, qtz = quartz.

K-feldspar crystals rimmed by plagioclase. On the other hand, the anti-rapakivi texture observed in thin section is characterized by reverse textural relationship where crystals of plagioclase are rimmed by K-feldspar. Plagioclase crystals mantled by a second plagioclase shell exhibits two distinct morphological features. One of the varieties is characterized by rectangular plagioclase rimmed by plagioclase displaying dendritic morphology (Figure 6 a,b). While the other variety is defined by plagioclase crystals surrounded by non-dendritic plagioclase (Figure 6 c,d).

The observed graphic texture comprises an intergrowth of quartz crystals within a K-feldspar host. The quartz associated with the graphic texture exhibits varying morphologies including triangular-shaped grains, quartz with lobate inner boundaries, and irregular boundaries. Sometimes, this texture is also found in association with the boundaries of dendritic plagioclase mantle on non-dendritic plagioclase (Figure 6 a,b). In this context, the crystals of quartz appear to be branching outwards from the associated plagioclase phenocrysts. Another notable textural feature observed in the thin sections is the presence of graphic texture mantled by plagioclase. The presence of such a mantling relationship between plagioclase and graphic texture is unique and has not been depicted in previous literature (Figure 5 c,d).

Mineral chemistry

Mineral chemistry studies were performed on K-feldspar, plagioclase, amphibole, and biotite, the four major mineral phases. These minerals' compositional analyses are included in Tables S1, S2, S3, and S4.

K-feldspar

K-feldspar compositions were determined from quartz

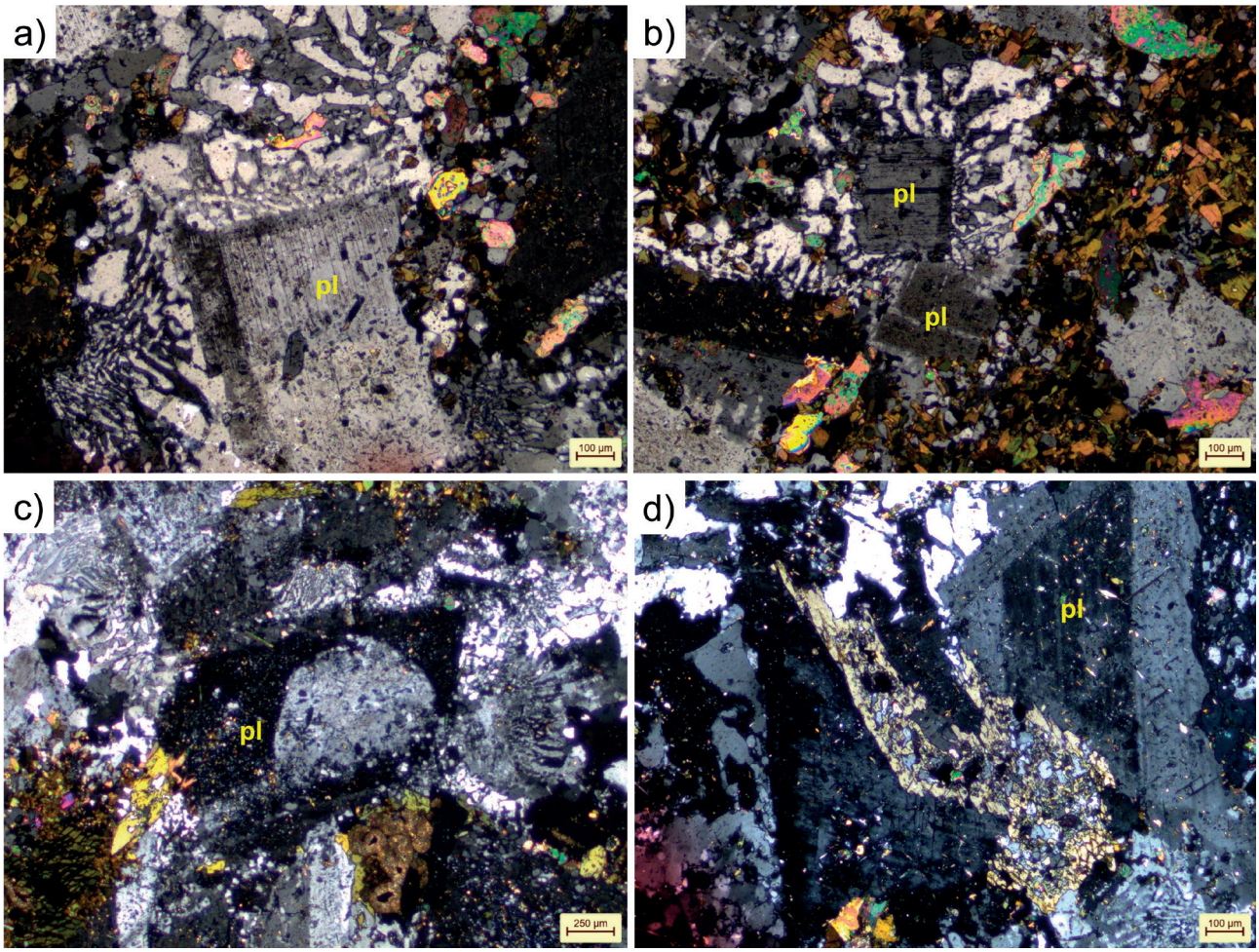

Figure 6. Detailed petrography of the studied samples. Crossed polars, transmitted light. a,b) Plagioclase mantled by dendritic plagioclase with adjoining graphic intergrowths. c,d) Zoned plagioclase having resorbed cores with euhedral rims. Abbreviation: pl = plagioclase.

graphic intergrowths depicting graphic texture, rapakivi feldspar, and anti-rapakivi feldspar. A total of 12 point analyses are reported for this mineral. The specific locations of point analyses are shown in Figure S3 and representative data are included in Table S1. Similar compositions have been observed in the K-feldspars from the three distinct zones, which plot in the field of orthoclase (Figure 7). The rapakivi and anti-rapakivi feldspar's K-feldspar is characterised by Or_{94-96}, while that occurring in the graphic texture is characterised by Or_{93-97}.

Plagioclase

Plagioclase compositions were determined from crystals mantling quartz graphic intergrowths, rapakivi and anti-rapakivi feldspars, crystals displaying dendritic overgrowth, and zoned crystals. A total of 22 point analyses are reported for this mineral. Representative data are included in Table S2 and the specific locations of point analyses are shown in Figure S3 and S4. Similar compositions have been observed in the plagioclases from the different zones, which mostly plot in the field of albite (Figure 7), except for 2 point analysis (one from anti-rapakivi feldspar and one from plagioclase showing dendritic overgrowth), which plot in the field of oligoclase.

Amphibole

Amphibole occurs as a major mineral phase in the dioritic rocks of the Borjuri Diorite Pluton. Amphibole present in these rocks is classified as Ca-amphibole based on the amphibole classification scheme of Leake et al. (1997). Compositions of amphibole plot in the field of hastingsite (Figure 8). The Ca contents in amphibole are in the range of 1.83-1.93 *apfu* (atoms per formula unit), Al^{iv} between 1.79-1.96 *apfu*, $(Na+K)_A$ between 0.62-0.72 *apfu*, and Mg# between 0.09-0.12 (Table S3).

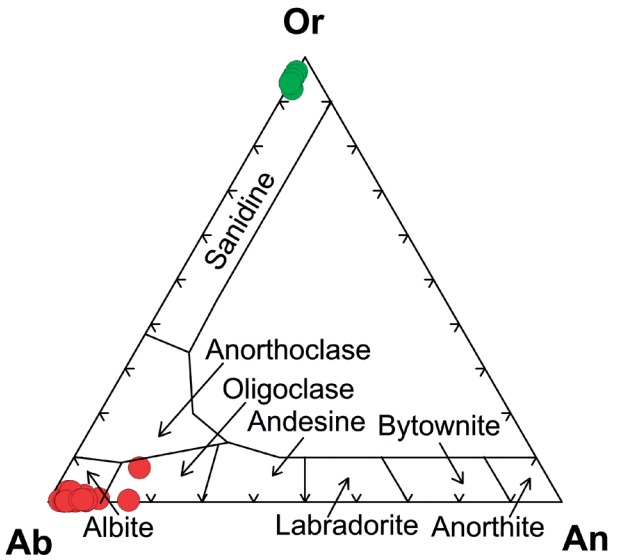

Figure 7. Nomenclature and classification of feldspar from the studied samples.

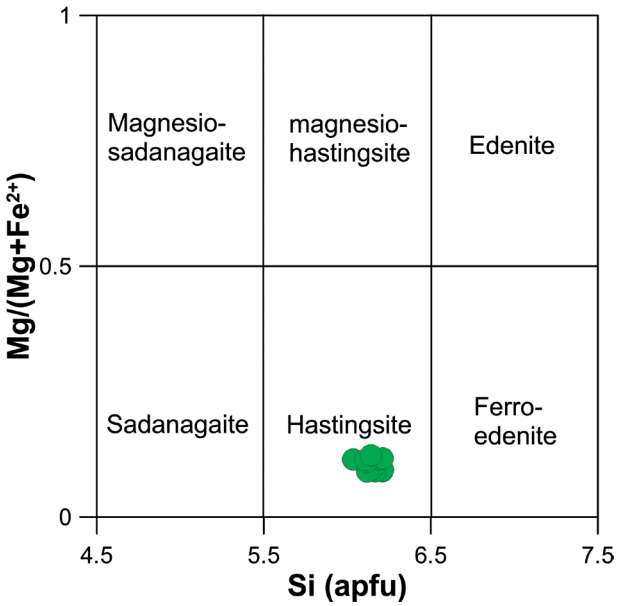

Figure 8. Nomenclature and classification of amphibole from the studied samples (after Leake et al., 1997).

Biotite

Biotite occurs as another major mineral phase in the dioritic rocks of the Borjuri Diorite Pluton. Biotite occurring in these rocks is classified as Fe-biotite and plots in the field of lepidomelane (Figure 9; Tischendorf et al., 1997). The Si values in biotite varies between 2.64- 2.79 *apfu*, total Al between 1.44-1.55 *apfu*, and Fe# between 0.85-0.87 (Table S4).

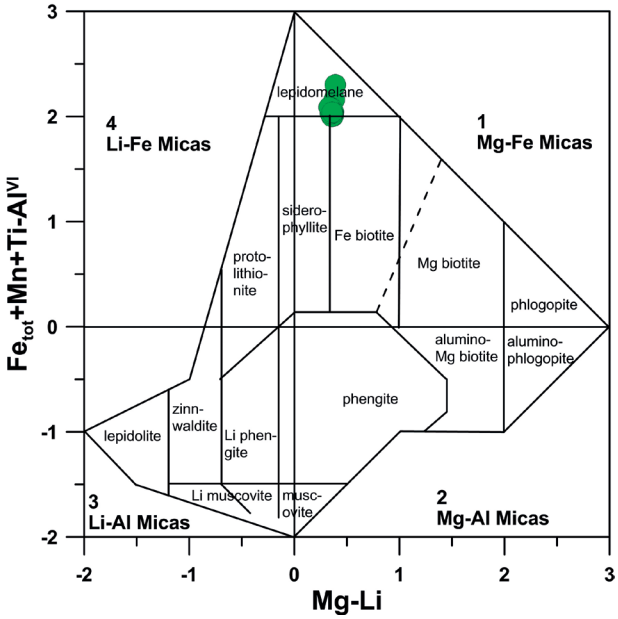

Figure 9. Nomenclature and classification of biotite from the studied samples (after Tischendorf et al., 1997).

Fractal and lacunarity calculations

Results of fractal and lacunarity calculations from cropped images of MD7, MD8, and MD28 are presented in Table S5. The negative trends of box-counting fractal dimensions (D_B) and lacunarity (Λ) plotted in Figure 10. Mutual relationship and distinct trends demonstrated by the values of D_B and Λ act as an indicator for deviation from equilibrium due to different stages of undercooling. Graphic intergrowths characterized by higher fractal dimensions, low lacunarity, and steep negative slope suggests greater extent of undercooling (deviation from equilibrium). With decreasing undercooling (closer to equilibrium), the fractal dimensions are low with increase in lacunarity values and flatter trends (Rusiecka and Baker, 2021). Taking into consideration the mutual relationship of fractal and lacunarity experimentally derived by Rusiecka and Baker, (2021), Figure 10 displays the measurements of D_B, Λ, and slope of the trends from the selected binary images of graphic intergrowths, which gives an impression of the different degrees of undercooling during crystallization. The parameters measured in the binary image of Sample MD7 depicting rod-shaped elongated grains (Figure 10a) form a trend with a higher negative slope (-1.013) with relatively higher box-counting fractal dimensions (1.75-1.83) and low lacunarity (0.17-0.26). The analyses of these parameters suggest that the sample MD7 likely originated under conditions of relatively higher degrees of undercooling. The measurements of D_B and Λ for sample MD8 with triangular arrow-headed

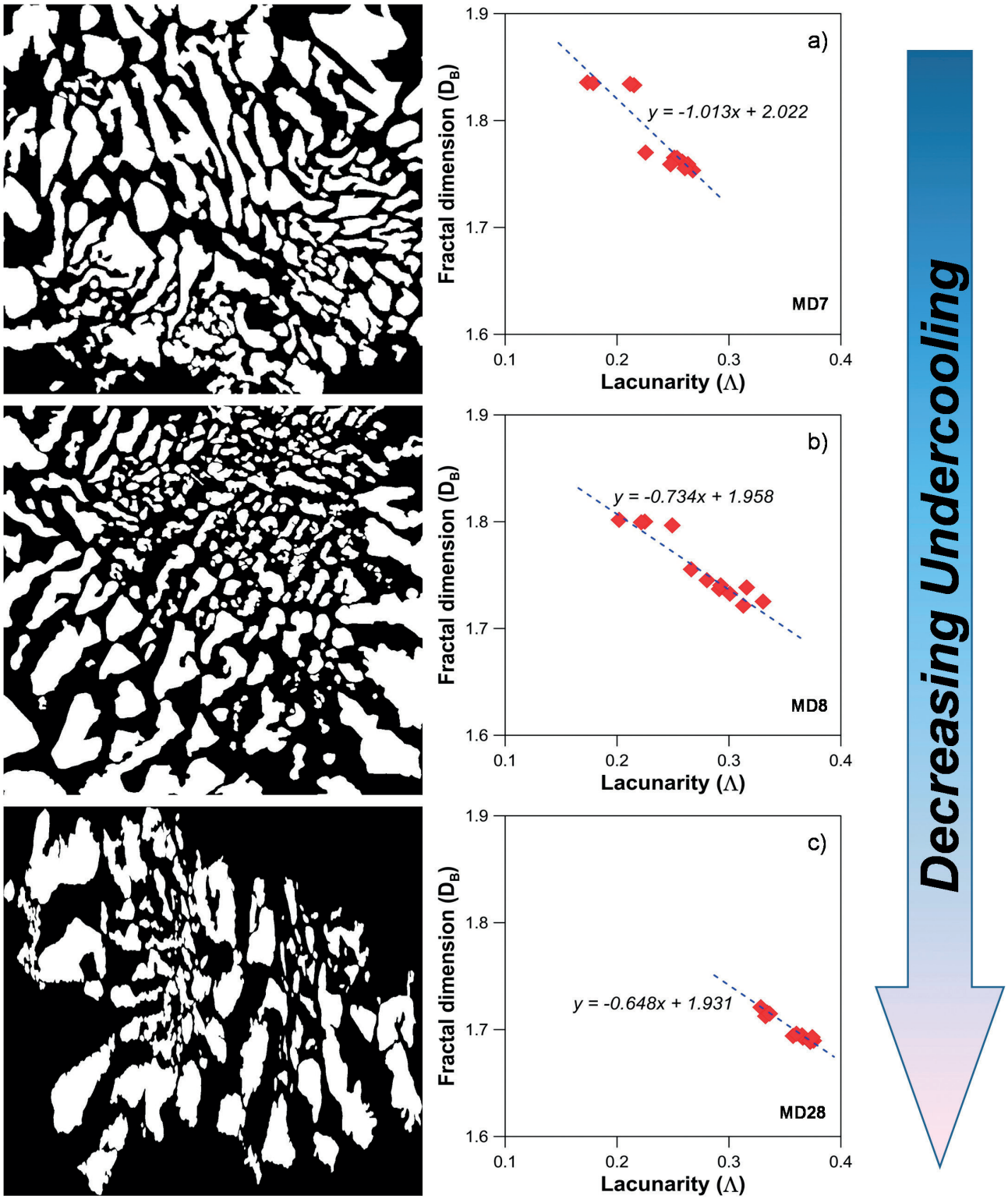

Figure 10. Representative binary images of the graphic intergrowths of different morphologies along with their respective graphs of D_B versus Λ formed under different degrees of undercooling. a) Intergrowths of quartz and feldspar with quartz showing rod like morphologies. b) Graphic intergrowths displaying triangular arrow headed quartz morphologies with distinct lobate boundaries. c) Graphic texture with coarser quartz grains and irregular boundaries.

morphology show relatively lesser fractal dimensions (1.72-1.80), higher lacunarity (0.20-0.33), and relatively lesser negative slope (-0.734) than MD7 (Figure 10b). With decreasing undercooling, the slope decreases and is characterized by lower fractal dimensions and high lacunarity. The measurements from binary image of sample MD28 representing coarser quartz grains with irregular boundaries display low D_B (1.67-1.71), high Λ (0.34-0.39), and comparatively lesser negative slope (-0.648) (Figure 10c).

DISCUSSION

Textural interpretations

Interpretation of variations in textures found in igneous rocks has the potential to provide important information on the physical history of the melt (Candela, 1997). Experimental verification of these textures provides qualitative information on various conditions responsible for crystal formation and degree of undercooling (Barker, 1970). Igneous rocks include abundant evidence of non-equilibrium crystal formation exhibited in the form of textural heterogeneity (Candela, 1997). The studied diorites show distinct disequilibrium textures identified through petrographic studies. This discussion focuses on the observed textures and elucidates the processes responsible for their formation.

Feldspar disequilibrium textures

Occurrence of disequilibrium textures in feldspars have been broadly observed and studied (Hibbard, 1981; Baxter and Feely, 2002). These textures occur essentially due to perturbations in a pre-existing state of equilibrium in a magmatic system. Existence of feldspar disequilibrium textures such as, rapakivi texture, anti-rapakivi texture, dendritic, and zoned plagioclase, also indicate mechanical mixing of felsic and mafic magmas. Understanding feldspars showing textural variations are crucial in understanding magmatic crystallization and have been reported in various literatures (Hibbard, 1981; Nakano, 2021). Hibbard (1981) put forward a model which suggests that variation of intensive variables (composition, temperature, and pressure) invoked during magma mixing favour the growth of atypical mantling textures. As per the model, such mixing of magmas leads to: (1) undercooling of the hotter, mafic magma and (2) superheating of the colder, felsic magma. The result is a quench texture which is basically epitaxial nucleation of plagioclase on K-feldspar or K-feldspar on plagioclase.

Rapakivi texture

Understanding the magmatic processes responsible for the generation of rapakivi feldspar offers significant insights regarding the evolution of the magmatic systems (Slaby and Gotze, 2004; Gogoi et al., 2020). The prime cause of the genesis of such mantled feldspars is epitaxial nucleation leading to crystal growth which subsequently yields rapakivi feldspars with a K-feldspar core and plagioclase mantle (Hibbard, 1981). The generation mechanism of this texture is still a subject of discussion and several researchers have presented their perspectives explaining the formation of their mantled nature. These include: i) Origin by sub-isothermal decompression. According to this model, decompression of felsic magma shifts the melt from K-feldspar stability field and enters plagioclase stability field. This results in mantling of plagioclase around the previously precipitated K-feldspar (Whitney, 1975). ii) Growth of rapakivi feldspars due to exsolution of plagioclase and its distribution around K-feldspar phenocrysts (Dempster, 1994). iii) Origin as a consequence of mixing of felsic magma rich in K-feldspar with magma of mafic nature. As a result of such interaction, the temperature of the felsic magma increases, which results in resorption of K-feldspar and nucleation of plagioclase rim around it (Hibbard, 1981; Slaby and Gotze, 2004). iv) Some studies have assigned the origin of rapakivi feldspar to a sudden loss of volatiles towards last stages of crystallization (Calzia and Ramo, 2005). Thus, several mechanisms may be accountable for the generation of rapakivi feldspars.

The rapakivi feldspars observed in the studied diorites are characterized by highly resorbed crystals of K-feldspar (Or_{95-96}) surrounded by plagioclase (An_{2-5}) (Figure 5 c,d; S2). Resorbed crystal formation is generally associated with two main mechanisms: increase in temperature due to magma mixing (Hibbard, 1981) or loss of volatiles (Stewart, 1959). Existence of disequilibrium textures; for instance, the presence of long prismatic apatites, skeletal morphology of amphibole, and biotite (mafic) clots is illustrative of rapid fluctuations in magma conditions owing to magma mixing (Vernon, 1983; Baxter and Feely, 2002; Campos et al., 2002). The presence of these disequilibrium textures suggest that magma mixing might be the underlying cause for the formation of resorbed crystals in our studied pluton. Thereby, we hypothesize that the generation of resorbed crystals in these rocks is the result of superheating caused by the intrusion of high-temperature mafic magma. Hence, in our study area, temperature perturbation owing to magma mixing might have triggered the resorption of K-feldspar crystals and the stabilization of plagioclase, some of which mantled on the K-feldspar crystals, leading to the formation of rapakivi feldspar.

Anti-rapakivi texture

Plagioclase mantled by K-feldspar has been studied in many plutonic and volcanic rocks, mostly from the latter.

However, there have been few reports on natural anti-rapakivi textures and studies have shown that peritectic reactions during fractional crystallization facilitate the development of such rare feldspars. Anti-rapakivi feldspars have been a subject of investigation since the pioneering work of Tuttle and Bowen (1958), particularly from the perspective of Or-Ab-An ternary feldspar phase relations. Following this work, Abbot (1978) also placed additional emphasis on a theoretical approach elucidating the formation of anti-rapakivi texture owing to peritectic reactions in the Or-Ab-An feldspar phase system. In the feldspar ternary projection, during ideal fractional crystallization, a melt cooling on the two-feldspar liquidus boundary deviates from the boundary with decreasing temperature. With further fractional crystallization, the melt will reach the peritectic point of the two-feldspar boundary and enter into K-feldspar liquidus field at lower temperatures.

Several studies have attributed the formation of anti-rapakivi feldspar to magma-mixing. In the granitoids of NE Turkey, Aslan and Aslaner (1998) observed anti-rapakivi feldspars in a series of quartz-monzodiorite, granodiorite and quartz-diorite. It is interesting to note here that the occurrence of anti-rapakivi texture was reported to be a consequence of mixing of two compositionally distinct magmas. Sarjoughian (2017) further reported anti-rapakivi texture from the Zafarghand complex in Iran and also suggested its formation to mafic-felsic magma mixing. Moreover, Gogoi et al. (2018) evaluated magma mixing in the subvolanic rocks of Ghansura Felsic Dome of Chotanagpur Granite Gneiss Complex, eastern India and also stated the presence of anti-rapakivi feldspars as evidence of magma mixing. Anti-rapakivi texture reported from Salto Rapakivi Granite, SE Brazil has also been considered to support magma mixing processes (Alves et al., 2021). Here in the current study, the anti-rapakivi feldspar observed in thin sections is characterized by crystals of plagioclase (An_{3-15}) mantled by K-feldspar (Or_{93-96}) (Figures 5 a,b, S3 c,d). Taking into consideration the results of earlier studies which analyzed the processes responsible for formation of anti-rapakivi texture, we have integrated our own interpretation to understand the processes responsible for its origin. Our study comes across a variety of disequilibrium textures thereby pointing towards an origin owing to magma mixing. Rapid lowering of temperature is a requisite for origin of anti-rapakivi feldspars. Thus, we speculate that rapid lowering of temperature for the generation of anti-rapakivi feldspars in our scenario was probably initiated by loss of volatiles due to magma mixing event.

Dendritic and zoned plagioclases

Igneous plagioclases are typically non-cellular, but rocks with mantled feldspars usually consists of cellular plagioclases, either as mantled or separate crystals (Hibbard, 1981). Lofgren (1974) stated that a dendritic crystal consists of crystallographic branches which are not necessarily of arborescent form. Experimental findings have shown that growth of such dendritic crystals is a function of marked undercooling. Rapid cooling is inevitable in volcanic environment and so is the formation of dendritic plagioclase. As such, occurrence of dendritic plagioclase in volcanic rocks is common. Significant heat loss by heat transfer to wallrocks in plutonic environment is unlikely, which results in non-cellular and coarse-grained textures. Equivalent quenching of magma systems, sufficient to grow cellular plagioclase can be achieved if felsic magma is abruptly mixed with mafic magma. Such magma mixing causes temporary thermal adjustment which yields a disequilibrium condition and nucleates dendritic plagioclase in coexisting plagioclase grains. Thus, dendritic plagioclases may be found in hybrid rocks resulting from magma mixing irrespective of their grain size. From petrographic observations, it is evident that dendritic plagioclases mantle around non-dendritic plagioclases (Figure 6 a,b, S4 a-c). The presence of such dendritic plagioclase and their mantling relationship is indicative of an undercooling phenomenon which was induced by magma mixing.

Zoning characteristics displayed by plagioclase crystals marks their growth in a magma mixing hybridization environment. In the mixing system, incorporation of mafic magma into a felsic magma system will cause reheating of the latter and further lead to resorption of sodic plagioclases. This is followed by nucleation of compositionally variant plagioclase around the resorbed crystals. The resorbed crystals have rounded corners and overgrowth rims tend to retain euhedral outline (Hibbard, 1981; Tepley et al., 1999). Zoned plagioclase grains with rounded resorbed cores and subhedral overgrowth rims were observed in the Borjuri diorites (Figure 6c, S4d). However, there is not much of a compositional difference between the core and the rim of the zoned plagioclase crystals.

Graphic intergrowth

Quartz found as intergrowths within K-feldspar host generally displays a cuneiform like appearance. Such textures are rarely found, and understanding the processes responsible for their formation are crucial in understanding the crystallization history of the rock (Fenn, 1986). Despite their sparse occurrence, many researchers have shed light regarding the origin of such graphic intergrowths. However, in due course of time, studies have tentatively underlined the involvement of rapid crystallization for such intergrowth textures. Earlier studies have

stressed upon the formation of graphic textures to be a consequence of simultaneous crystallization of quartz and feldspar (Barker, 1970). Eventually, the subject of debate has shifted on the importance of undercooling for the development of graphic intergrowths (Candela, 1997; Rusiecka and Baker, 2021). Undercooling defines the difference between melt saturation temperature with respect to a mineral and the temperature at which nucleation initiates in a mineral. Hence, a deviation from the equilibrium initiated by undercooling contributes to the formation of such intergrowth texture.

The observed graphic textures are of variable nature and are characterized by different morphologies of quartz crystals (Figure 10, S5). This paper aims to implement fractal and lacunarity calculations to qualitatively suggest that variations in quartz graphic morphologies may be attributed to different degrees of undercooling. The grain size of the texture, i.e., the average distance between the quartz domains can be defined as medium to coarse grained. The quartz crystals display triangular, rod-like, and irregular boundaries showing evidence of change in morphology owing to different stages of undercooling. The quartz grains moreover depict lobate inner boundaries in some of the crystals (Figure 10b, S5b). The observations of such lobate boundaries are crucial as they define conditions of high supercooling. Such conditions are interpreted to arise due to low diffusivities in the boundary layer owing to non-equilibrium growth (Woodruff, 1973). Graphic intergrowths are found generously distributed throughout the samples. However, some of these intergrowths are also found in association with plagioclase phenocrysts (Figure 6 a,b). The quartz crystals nucleating from the boundary of the phenocrysts are finer in nature with them attaining a coarser nature away from the associated phenocryst. The finer quartz grains have higher fractal dimensions ranging from 1.79 to 1.86 and lower lacunarity values ranging from 0.17 to 0.25. On the contrary, the coarser variety of quartz grains have lower fractal dimensions (1.71 to 1.77) and higher values of lacunarity (0.30 to 0.38). Furthermore, in the plagioclase phenocrysts mantled by dendritic plagioclase, the graphic intergrowths seem to have nucleated from the boundary of the mantled dendritic plagioclase (Figure 11 b,c). An interesting feature observed in the study is the presence of plagioclase overgrowth on quartz graphic intergrowths (Figure 11d). This is possibly the first report of such an assemblage. Here, we propose that the formation of quartz graphic intergrowths occurred due to undercooling in the magmatic system brought about by a sudden rise in liquidus temperature of the magma. The overgrowth of plagioclase on the quartz graphic intergrowths formed when the magmatic system re-equilibrated to its thermodynamic equilibrium.

Understanding the effect of undercooling on graphic intergrowth (fractal and lacunarity calculations)

The process of magma crystallization is governed by nucleation and crystal growth kinetics, with fundamental concepts concerning these factors established long ago to explain the crystallization of magma (Tammann, 1925). Nucleation includes incorporating atoms or molecules into a nucleus, which is the initial step in the formation of a crystal (Swanson, 1977). If the nucleus exceeds a certain critical size, it will develop spontaneously, but if it remains below that size, it will become unstable. The critical size is influenced by the amount of undercooling and can range from infinite at liquidus temperature to progressively smaller sizes as the undercooling increases (Swanson, 1977). Crystal morphology describes the shape of individual crystals, which is influenced by the growth rate and vary with undercooling (Kirkpatrick, 1975). Given that both nucleation and growth rate are affected by undercooling, textures are expected to vary accordingly. The observed textures are thus used to interpret the extent of undercooling undergone by the rock (Winter, 2001). A lesser degree of undercooling causes a low nucleation rate and accelerated growth rate, resulting in fewer coarse-grained crystals. In case of high degrees of undercooling, the nucleation rate surpasses the growth rate, resulting in the development of many fine-grained crystals (Fenn, 1977; Bouloton and Gasquet, 1995).

In the present study, the quartz graphic intergrowth texture developed from the melt of dioritic composition display different morphologies, as they were produced at different stages of undercooling. Characteristic quartz morphologies and sizes encountered in this study include small triangular arrow-headed grains with lobate quartz-feldspar interface, rod-shaped elongated grains, and anhedral grains with irregular boundaries (Figure S5). In this study, the complexity of the quartz assemblages is measured in terms of box-counting fractal dimensions (D_B). The heterogeneities in texture defined by quartz within the binary images are measured in terms of lacunarity (Λ) (Figure 10). On the basis of the possible relationship between fractal dimension and lacunarity experimentally found by Rusiecka and Baker (2021), we infer the variation in undercooling from the binary images. The parameters calculated from the binary images MD7 and MD8 (Figure 10 a,b), having relatively finer quartz crystals show a steep negative slope, indicating that they likely formed under higher undercooling conditions. In contrast, MD28 (Figure 10c) having coarser quartz-grains show smaller fractal dimensions and higher lacunarity, and a relatively flatter trend.

Volatile saturation after rise of undersaturated volatiles prompts the growth of disequilibrium textures (e.g. skeletal quartz). Eventually, with further rise of magma,

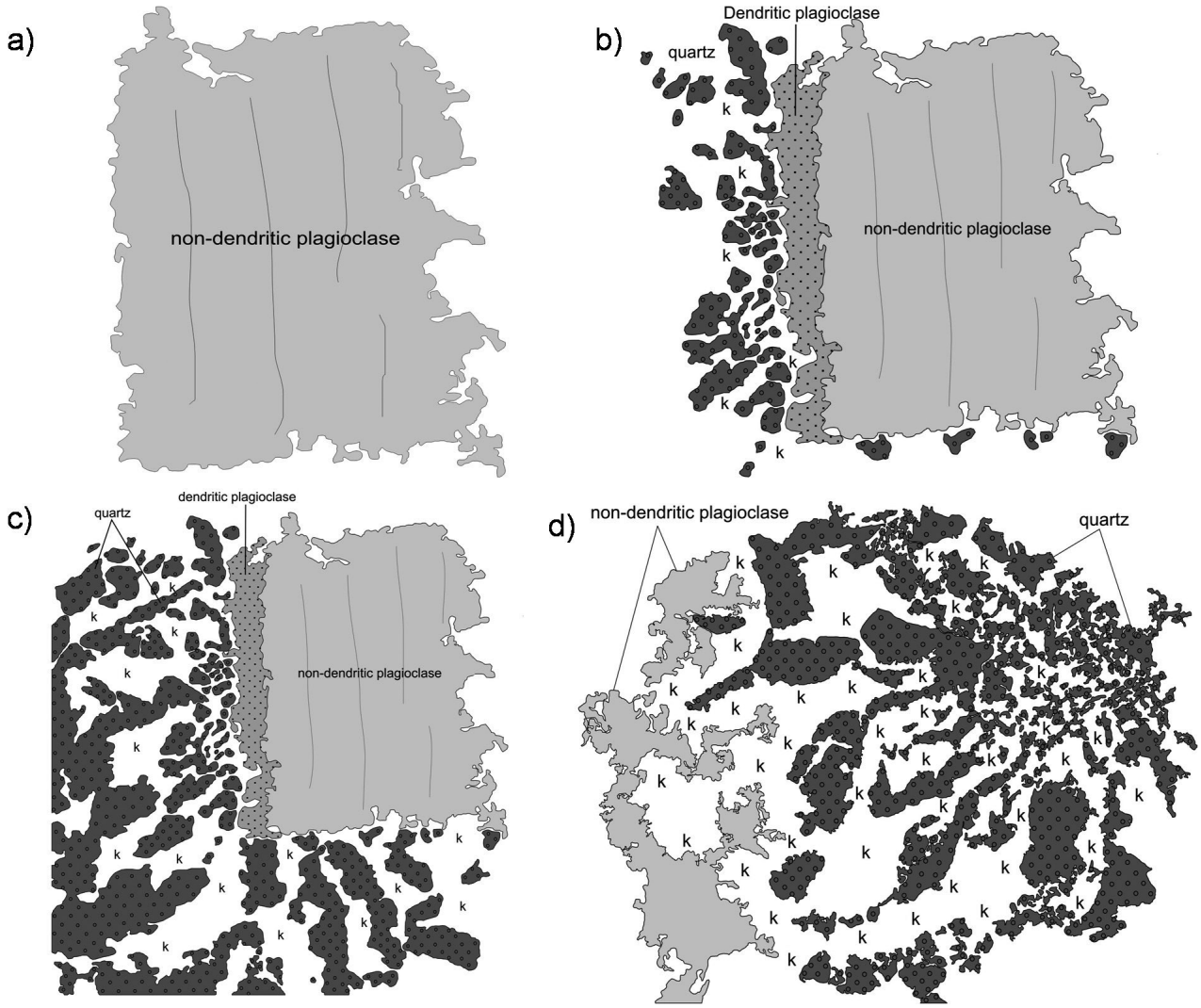

Figure 11. Schematic representation of disequilibrium texture formation reflecting differing undercooling conditions. a) Coarse-grained non-dendritic plagioclase crystal development under normal equilibrium conditions. b) Dendritic plagioclase mantling the plagioclase phenocryst with fine-grained graphic intergrowths near the phenocryst indicating a sudden undercooling phenomenon. c) Development of coarse-grained quartz crystals away from the phenocryst with gradual decrease in undercooling. d) Graphic texture mantled by non-dendritic plagioclase indicating re-equilibration of the magmatic system.

undercooling increases and skeletal quartz are overgrown by quartz of dendritic nature. Such dendritic forms may be seen either in the groundmass or around pre-existing phenocrysts (Ratajeski, 1995). It is noteworthy that some of the graphic intergrowths seem to emerge from the boundaries of plagioclase phenocrysts (Figure 6 a,b). In this study, the graphic intergrowths found around the plagioclase phenocrysts seem to be finer near the margin of the phenocrysts and eventually attaining a more outward branching dendritic nature away from the phenocrysts (Figure 12). Comparing the fractal dimensions and lacunarity of both the finer and coarser quartz grains suggests a possible variation in the degree of undercooling away from the phenocryst. The quartz grains nucleating from the boundary of the plagioclase phenocryst are finer and display higher fractal dimensions (1.79-1.86) with lower values of lacunarity (0.17-0.25). These evaluations along with a high negative slope (-0.88) indicate a greater degree of undercooling. On the other hand, the bigger quartz crystals situated farther from the phenocryst, creates an outward branching distinct dendritic pattern. The values of fractal dimensions (1.71-1.77), lacunarity

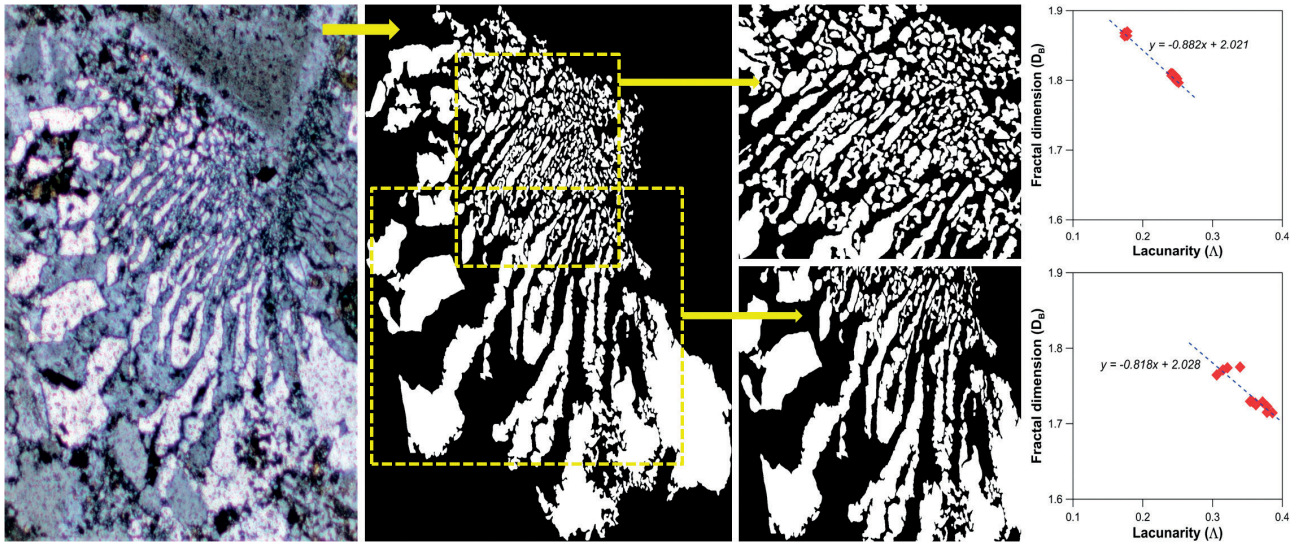

Figure 12. Original photomicrograph of graphic intergrowths associated with plagioclase phenocryst (on the left), followed by its binary image. The areas selected for measurement is demarcated by the yellow rectangles. The changing morphology of the quartz crystals (from fine to coarse) is demonstrated by their respective graphs of D_B versus Λ.

(0.30-0.38), and relatively lower negative slope (-0.81) contrasts with the fine-grained quartz which are in closer proximity to the phenocryst.

The fractal dimensions and lacunarity of various morphologies demonstrated in Figure 10 and Figure 12 were compared (Figure 13). It is to be noted here that the variation in extent of undercooling controls the change in morphology of quartz crystals of the graphic intergrowth. The Borjuri diorite pluton formed under plutonic conditions, where coarse-grained non-dendritic

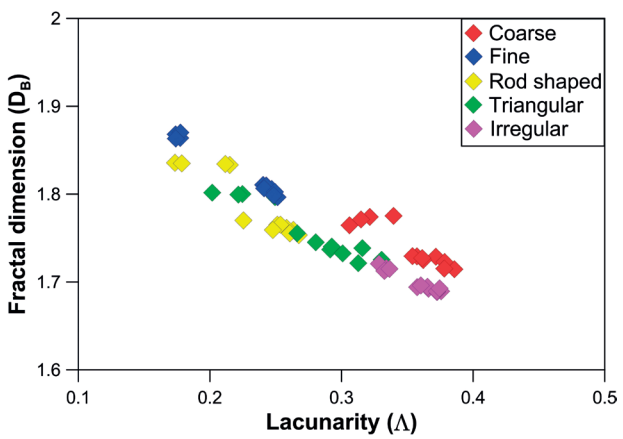

Figure 13. Box-counting fractal dimension versus lacunarity of the quartz-feldspar intergrowths having different morphologies. The varying morphologies display a negative trend signifying their formations at different degrees of undercooling.

plagioclase crystals crystallized under normal equilibrium conditions (Figure 11a). However, a sudden undercooling event disrupted this equilibrium, which resulted in the crystallization of dendritic plagioclase mantling the plagioclase phenocryst, along with fine-grained quartz graphic intergrowth near the phenocryst (Figure 11b). With gradual decrease in undercooling, the quartz grains from the quartz graphic intergrowth became progressively coarser (Figure 11c). Subsequently, the final stage involved mantling of non-dendritic plagioclase on graphic texture which clearly indicates that the magmatic system has re-equilibrated to its original state (Figure 11d). The fine-grained quartz likely formed due to higher degree of undercooling, displays a morphology similar to rod-shaped and triangular arrow-headed grains. Also, some graphic intergrowths displaying triangular grains and quartz grains with irregular boundaries, are formed due to decrease in undercooling, as indicated by fractal and lacunarity calculations (Figure 13).

Magma mixing-induced undercooling

Input of hotter mafic magma into a reservoir hosting cooler felsic magma may lead to the addition of heat, mass, and/or volatiles to the felsic magma reservoir. Influx of mantle-derived mafic magmas into crystallizing granitic magma chambers is a common phenomenon, which may bring about a wide range of physical and chemical interactions between the mafic and felsic magmas. Processes like magma mixing plays a major role in changing the thermal history of the melt (Hort,

1998). The liquidus temperature in a melt may change abruptly due to release of volatiles or due to mixing of magmas or a combination of both. When a magma of basaltic composition (mafic magma) enters into a felsic magma chamber, certain physical processes are initiated in the latter: (1) superheating of the felsic magma (Sparks et al., 1977; Snyder, 1997) (2) convection in the magma chamber (Sparks et al., 1977) (3) volatile transfer from the mafic to the felsic magma (Sparks et al., 1977; Murphy et al., 1998; Kazahaya et al., 2002) (4) reduction in viscosity of the felsic magma (Ruprecht and Bachmann, 2010) (5) volatile exsolution and degassing in the magma chamber (Sparks et al., 1977; Ruprecht and Bachmann, 2010). In our scenario, the Borjuri diorite pluton was a crystallizing granitic magma chamber that was intruded by mantle-derived mafic magma leading to superheating of the felsic magma and convection in the magma reservoir. Evidence of superheating is preserved in the K-feldspar cores of rapakivi feldspars that have undergone strong resorption (Figure 5 c,d, S2). The resorbed K-feldspar cores represent earlier crystallizing K-feldspar crystals in the felsic magma that underwent resorption due to superheating of the felsic magma by the intruding mafic magma (Hibbard, 1981). Evidence of convection within the magma reservoir is supported by the homogeneous nature of the dioritic rocks (Figure 3), as vigorous convective stirring is essential to bring about complete blending or hybridization of the mafic and felsic magmas to produce a homogeneous hybrid rock of intermediate composition (Oldenburg, 1989; Perugini and Poli, 2004; Morgavi et al., 2012). The combination of two processes after intrusion of the mafic magma into the felsic magma chamber, i.e. superheating and convection, led to supersaturation of saturated volatile phases causing them to exsolve into vapour bubbles (Sparks et al., 1977; Snyder, 1997). Superheating or reheating of the felsic magma following magma mixing leads to lowering of viscosity and accelerates volatile diffusion, which in turn facilitates bubble nucleation, growth, and coalescence, ultimately leading to magma degassing (Ruprecht and Bachman, 2012). Such volatile exsolution mostly takes place when the level of saturation is reached. Degassing has significant effects on magmatic phase equilibria and crystallization, and as such degassing has proved to be of great significance (Sparks, 2003). Crystallization due to volatile exsolution (mainly H_2O) involves perturbations in liquidus temperatures which sheds light on the magmatic processes that take place. Such crystal growth and nucleation are also elaborated in terms of increased undercooling due to increase in liquidus temperature following magma degassing. Hort (1998) explained this undercooling effect below the liquidus as a possible outcome of volatile exsolution due to magma mixing. It has to be noted here that exsolution of volatile phases or vesiculation significantly increases the pressure within the magma chamber (Sparks et al., 1977). The overpressure created may be dispersed by volatile loss or magma degassing via dykes emerging from the magma chamber (Underwood et al., 2012).

Regional geodynamic setting

The Borjuri diorite pluton, emplaced in the Mikir Massif of Assam-Meghalaya Gneissic Complex (AMGC), is a product of Pan-African post-collisional intermediate magmatism (Prakash et al., 2023). Numerous Pan-African granitic plutons, such as Mylliem, Kyrdem, South Khasi, Nongpoh, Sonsak, Kathalguri, Kaziranga, and Bamuni are widely distributed in the AMGC. Reports from Mylliem, Nongpoh, and South Khasi plutons from the Shillong Plateau of AMGC confirm the role of magma mixing in their magmatic evolution (Kumar et al., 2017; Sadiq et al., 2017; Choudhury and Hussain, 2021). Magma mixing has also been reported from the Kathalguri and Bamuni granite plutons of Mikir Massif, which are present in close proximity with the Borjuri diorite pluton (Figure 2; Hazarika et al., 2022; Hazarika and Gogoi, 2023; Hazarika et al., in preparation). Thus, Pan-African magmatism in the AMGC is generally characterised by granitic plutons, which were frequently intruded by mantle-derived mafic magmas during their evolution. The Borjuri pluton is the first and only occurrence of a diorite pluton in the AMGC (Prakash et al., 2023). From a regional perspective, the current investigation reports a distinctive occurrence of magma mixing within a diorite pluton.

Diorite magmatism can be attributed to: i) partial melting of crustal rocks (McDermott et al., 1996), ii) fractional crystallization of mantle-derived mafic magmas (Jiang et al., 2002), and iii) mixing of felsic and mafic magmas (Wang et al., 2013). Elemental ratios such as Rb/Sr, La/Nb, and Nb/Ce along with SiO_2 versus Mg# binary diagram derived in the previous report of the Borjuri diorite pluton suggest that the diorites have a crustal origin (Prakash et al., 2023). Moreover, values of Mg# and elemental ratios like Zr/Nb and La/Sm, indicate the involvement of partial melting of crustal rocks in the formation of the diorites. In our opinion, partial melting of crustal components alone is unlikely to be accountable for the generation of these intermediate rocks hosting a variety of magma mixing signatures, specifically different varieties of mantled feldspars as described by Hibbard (1981). There must be some amount of mafic input in order to generate such rock types. Our study supports the hypothesis that the diorites under investigation originated from a magma mixing process, wherein the interaction of both felsic and mafic magmas played an essential role in the formation of intermediate rocks. Mafic magma

intrusion into a crustal magma chamber initiated magma mixing and resulted in formation of the intermediate Borjuri diorites.

CONCLUSIONS

From our observations, along with the integrated results, we have come across the following conclusions which add further insights into the graphic intergrowth texture:

(i) This study sheds light on the role of magma mixing, which in turn controls the effective undercooling for the formation of graphic intergrowths. The abrupt liquidus change (undercooling) is instigated due to devolatilization as a result of mixing between two compositionally distinct magmas. The initiation of undercooling for the origin of graphic texture involves more than one mechanism. Hence, effort should be given on amalgamation of these mechanisms for a more complete approach.

(ii) Fractal and lacunarity calculations were used to estimate the complexity of the graphic intergrowths which in turn gives a qualitative assessment of the relative change in undercooling on the basis of a correlation provided by a previous experiment. We have observed different morphologies depicted by quartz crystals such as arrow-headed, rod-shaped, and irregular boundary in the graphic texture and based on the trends shown by the fractal and lacunarity values of different morphologies of quartz, we consider that the morphological variations might be due to changing undercooling conditions.

(iii) Graphic intergrowths accompanied by mantled feldspars are unique and have not yet been reported. The presence of such mantled feldspars along with significant disequilibrium textures decipher the involvement of magma mixing in the studied samples. Additionally, the presence of mantled plagioclase on graphic intergrowths is another new feature which is speculated to result when the magmatic system re-equilibrated post undercooling.

(iv) Pan-African granitic plutons from the AMGC validate the role of magma mixing in their evolutionary process. The Borjuri diorite pluton represents the sole occurrence of diorite magmatism in the AMGC. The current study suggests that magma mixing plays a significant role in the generation of intermediate magmas.

ACKNOWLEDGEMENTS

The authors are grateful to Prof. Suresh Chandra Patel, Dr. Prabhakar Naraga, and Mr. Javed M. Shaikh for EPMA analyses at the Department of Earth Sciences, IIT Bombay. We are grateful to Prof. Ewa Slaby for the useful suggestions in shaping the manuscript. The authors are very grateful to an anonymous reviewer for an in-depth and constructive review which greatly improved the quality of the manuscript. We thank Prof. Paolo Ballirano and Prof. Alessandro Vona for editorial handling of the manuscript. BG acknowledges the DST-SERB grant vide Project No. CRG/2020/002635. PB acknowledges the CSIR-JRF fellowship No. 09/1236(11154)/2021-EMR-I.

REFERENCES

Abbott R.N., 1978. Peritectic reactions in the system An-Ab-Or-Qz-H2O. Canadian Mineralogist 16, 245-256.

Alves A., de Assis Janasi V., de Souza Pereira G., Prado F.A., Munoz P.R., 2021. Unravelling the hidden evidences of magma mixing processes via combination of in situ Sr isotopes and trace elements analyses on plagioclase crystals. Lithos 404, 106435.

Aslan Z. and Aslaner M., 1998. Evidence of magma mixing and hybrid source on calc-alkaline Saruhan (Bayburt) Granitoid, NE Turkey. Mineralogical Magazine A 62, 79-80.

Barker D.S., 1970. Compositions of granophyre, myrmekite, and graphic granite. Geological Society of America Bulletin 81, 3339-3350.

Basumatary P., Saikia A., Prakash T., Gogoi B., 2023. Geochemical constraints on the petrogenesis of mafic rocks (metadolerites) from the Proterozoic Shillong Basin, Northeast India: implications for growth of the Greater Indian Landmass. Geological Magazine 160, 1114-1130.

Baxter S. and Feely M., 2002. Magma mixing and mingling textures in granitoids: examples from the Galway Granite, Connemara, Ireland. Mineralogy and Petrology 76, 63-74.

Bhattcharjee C. and Rahman S., 1985. Structure and lithostratigraphay of the Shillong Group of rocks of East Khasi Hills of Meghalaya. Bulletin Geological Mining Metalurgical Society of India 53, 90-99.

Borah D., Chauhan H., Saikia A., Gogoi B., 2023. Petrogenesis of high-Mg andesites from the Proterozoic Shillong Basin, Northeast India: evidence for continuation of the Central Indian Tectonic Zone to the Assam-Meghalaya Gneissic Complex and its implications for the Columbia supercontinent reconstruction. International Geology Review, 1-21.

Calzia J.P. and Rämö O.T., 2005. Miocene rapakivi granites in the southern Death Valley region, California, USA. Earth-Science Reviews 73, 221-243.

Campos T.F.C., Neiva A.M.R., Nardi L.V.S., 2002. Geochemistry of the Rio Espinharas hybrid complex, northeastern Brazil. Lithos 64(3-4), 131-153.

Candela P.A., 1997. A review of shallow, ore-related granites: textures, volatiles, and ore metals. Journal of petrology 38, 1619-1633.

Choudhury D. and Hussain M.F., 2021. Neoproterozoic highly fractionated I-type granitoids of Shillong Plateau, Meghalaya, Northeast India: geochemical constraints on their petrogenesis. Acta Geochimica 40, 51-66.

Dempster T.J., Jenkin G.R.T., Rogers G., 1994. The origin of rapakivi texture. Journal of Petrology 35, 963-981.

Dhurandhar A.P., Pandey U.K., Raminaidu C., 2019. Petrochemistry and Sr, Nd, Pb Isotopic Characteristics of

Basic Dykes of Mikir Hills, Assam. Journal of the Geological Society of India 94, 559-572.

Fenn P.M., 1986. On the origin of graphic granite. American Mineralogist 71, 325-330.

Fowler A.D., 1995. Mineral crystallinity in igneous rocks: Fractal method. Fractals in the earth sciences, 237-249.

Ghosh S., Fallick A.E., Paul D.K., Potts P.J., 2005. Geochemistry and origin of Neoproterozoic granitoids of Meghalaya, Northeast India: Implications for linkage with amalgamation of Gondwana supercontinent. Gondwana Research 8, 421-432.

Gogoi A., Majumdar D., Cottle J., Dutta P., 2019. Geochronology and geochemistry of Mesoproterozoic porphyry granitoids in the northern Karbi Hills, NE India: Implications for early tectonic evolution of the Karbi Massif. Journal of Asian Earth Sciences 179, 65-79.

Gogoi B., 2022. Late Paleoproterozoic bimodal magmatic rocks in the Nimchak Granite Pluton of the Bathani volcano-sedimentary sequence, Eastern India: implications for the Columbia supercontinent formation with respect to the Indian landmass. Periodico di Mineralogia 91, 1-20.

Gogoi B., Chauhan H., Saikia A., 2020. Understanding mafic-felsic magma interactions in a subvolcanic magma chamber using rapakivi feldspar: A case study from the Bathani volcano-sedimentary sequence, eastern India. Geochemistry 81, 125730.

Gogoi B., Saikia A., Ahmad M., Ahmad T., 2018. Evaluation of magma mixing in the subvolcanic rocks of Ghansura Felsic Dome of Chotanagpur Granite Gneiss Complex, eastern India. Mineralogy and Petrology 112, 393-413.

Hazarika G., Chauhan H., Khandelwal D., Pandey A.C., Saikia A., Gogoi B., 2024. HR-SIMS U-Pb geochronology and petrogenesis of the Bamuni Pluton, Mikir Massif, Northeast India: implications for final assembly of the eastern Gondwana landmass. (in preparation).

Hazarika G. and Gogoi B., 2023. Fractal analysis and geochemical characterization of mafic magmatic enclaves in the Kathalguri Pluton, Mikir Massif (Northeast India): implications for Pan-African bimodal magmatism. International Journal of Earth Sciences 112, 685-705.

Hazarika G., Basumatary P., Prakash T., Chauhan H., Gogoi B., 2022. Magma mixing dynamics in a vertically zoned granitic magma chamber inferred from feldspar disequilibrium assemblage and biotite composition: a case study from the Mikir Massif, eastern India. Acta Geochimica 41, 453-469.

Hibbard M.J., 1980. Indigenous source of late-stage dikes and veins in granitic plutons. Economic Geology 75, 410-423.

Hibbard M.J., 1981. The magma mixing origin of mantled feldspars. Contributions to Mineralogy and Petrology 76, 158-170.

Hort M., 1998. Abrupt change in magma liquidus temperature because of volatile loss or magma mixing: effects on nucleation, crystal growth and thermal history of the magma. Journal of Petrology 39, 1063-1076.

Hughes C.J., 1971. Anatomy of a granophyre intrusion. Lithos 4, 403-415.

Jiang Y.H., Jiang S.Y., Ling H.F., Zhou X.R., Rui X.J., Yang W.Z., 2002. Petrology and geochemistry of shoshonitic plutons from the western Kunlun orogenic belt, Xinjiang, northwestern China: implications for granitoid geneses. Lithos 63(3-4), 165-187.

Karperien A., 2013. FracLac for ImageJ. Introduction.

Kazahaya K., Shinohara H., Saito G., 2002. Degassing process of Satsuma-Iwojima volcano, Japan: Supply of volatile components from a deep magma chamber. Earth, planets and space 54, 327-335.

Kumar S., Pieru T., Rino V., Hayasaka Y., 2017. Geochemistry and U-Pb SHRIMP zircon geochronology of microgranular enclaves and host granitoids from the South Khasi Hills of the Meghalaya Plateau, NE India: evidence of synchronous mafic-felsic magma mixing-fractionation and diffusion in a post-collision tectonic environment during the Pan-African orogenic cycle. Geological Society, London, Special Publications 457, 253-289.

Leake B.E., Woolley A.R., Arps C.E., Birch W.D., Gilbert M.C., Grice J.D., Youzhi G., 1997. Nomenclature of amphiboles; report of the subcommittee on amphiboles of the International Mineralogical Association, Commission on New Minerals and Mineral Names. The Canadian Mineralogist 35, 219-246.

Lofgren G., 1974. An experimental study of plagioclase crystal morphology; isothermal crystallization. American journal of Science 274, 243-273.

London D., Morgan G.B., Hervig R.L., 1989. Vapor-undersaturated experiments with Macusani glass+ H_2O at 200 MPa, and the internal differentiation of granitic pegmatites. Contributions to Mineralogy and Petrology 102, 1-17.

MacLellan H.E. and Trembath L.T., 1991. The role of quartz crystallization in the development and preservation of igneous texture in granitic rocks; experimental evidence at 1 kbar. American Mineralogist 76, 1291-1305.

Majumdar D. and Dutta P., 2016. Geodynamic evolution of a Pan-African granitoid of extended Dizo Valley in Karbi Hills, NE India: evidence from geochemistry and isotope geology. Journal of Asian Earth Sciences 117, 256-268.

Mandelbrot B.B., 1982. The fractal geometry of nature. San Francisco, 480.

Martin R.F., 1982. Quartz and feldspars. In Granitic Pegmatites in Science and Industry (P.Cerny, Ed.). Mineralogical Association of Canada: Short Course Handbook 8, 41-62.

McDermott F., Harris N.B.W., Hawkesworth C.J., 1996. Geochemical constraints on crustal anatexis: a case study from the Pan-African Damara granitoids of Namibia. Contributions to Mineralogy and Petrology 123, 406-423.

Morgavi D., Perugini D., De Campos C.P., Ertl-Ingrisch W., Lavallée Y., Morgan L., Dingwell D.B., 2012. Interactions between rhyolitic and basaltic melts unraveled by chaotic

mixing experiments. Chemical Geology 346, 199-212.

Murphy M.D., Sparks R.S.J., Barclay J., Carroll M.R., Lejeune A.M., Brewer T.S., Young S., 1998. The role of magma mixing in triggering the current eruption at the Soufriere Hills volcano, Montserrat, West Indies. Geophysical Research Letters 25, 3433-3436.

Nakano S., 2021. Magmatic crystallization processes inferred from microtextures in anti-rapakivi feldspars: A case study of ferro-augite trachyte feldspars from Oki-Dogo, Japan. Lithos 398, 106288.

Nandy D.R., 2001. Geodynamics of Northeastern India and the adjoining region. ACB Publications, Kolkata.

Oldenburg C.M., Spera F.J., Yuen D.A., Sewell G., 1989. Dynamic mixing in magma bodies: theory, simulations and implications. Journal of Geophysical Research 94, 9215-9236.

Perugini D. and Poli G., 2004. Analysis and numerical simulation of chaotic advection and chemical diffusion during magma mixing: petrological implications. Lithos 78, 43-66.

Perugini D., Poli G., Mazzuoli R., 2003. Chaotic advection, fractals and diffusion during mixing of magmas: evidence from lava flows. Journal of Volcanology and Geothermal Research 124, 255-279.

Prakash T., Saikia A., Basumatary P., Gogoi B., 2023. Petrogenesis of the Borjuri diorite pluton in the Mikir Massif of Northeast India: implications for post-collisional intermediate magmatism during the Pan-African orogeny. Acta Geochimica 42, 747-764.

Ratajeski K., 1995. Estimation of initial and saturation water concentrations for three granitic plutons in the north-central Great Basin, Nevada. Doctoral dissertation, University of Maryland at College Park).

Ruprecht P. and Bachmann O., 2010. Pre-eruptive reheating during magma mixing at Quizapu volcano and the implications for the explosiveness of silicic arc volcanoes. Geology 38, 919-922.

Rusiecka M.K. and Baker D.R., 2021. Growth and textural evolution during crystallization of quartz and feldspar in hydrous, rhyolitic melt. Contributions to Mineralogy and Petrology 176(7), 48.

Sadiq M., Umrao R.K., Sharma B.B., Chakraborti S., Bhattacharyya S., Kundu A., 2017. Mineralogy, geochemistry and geochronology of mafic magmatic enclaves and their significance in evolution of Nongpoh granitoids, Meghalaya, NE India. Geological Society, London, Special Publications 463, 171-198.

Sarjoughian F., Lentz D., Kananian A., Ao S., Xiao W., 2017. Geochemical and isotopic constraints on the role of juvenile crust and magma mixing in the UDMA magmatism, Iran: evidence from mafic microgranular enclaves and cogenetic granitoids in the Zafarghand igneous complex. International Journal of Earth Sciences 107, 1127-1151.

Słaby E. and Götze J., 2004. Feldspar crystallization under magma-mixing conditions shown by cathodoluminescence and geochemical modelling-a case study from the Karkonosze pluton (SW Poland). Mineralogical Magazine 68, 561-577.

Słaby E., Martin H., Hamada M., Śmigielski M., Domonik A., Götze J., Jayananda M., 2012. Evidence in Archaean alkali feldspar megacrysts for high-temperature interaction with mantle fluids. Journal of Petrology 53, 67-98.

Smith Jr T.G., Lange G.D., Marks W.B., 1996. Fractal methods and results in cellular morphology-dimensions, lacunarity and multifractals. Journal of neuroscience methods 69, 123-136.

Smith J.V., 1974. Feldspar minerals: 2 chemical and textural properties. Springer-Verlag, New York.

Snyder D., 1997. The mixing and mingling of magmas. Endeavour 21, 19-22.

Sparks R.S.J., 2003. Dynamics of magma degassing. Geological Society, London, Special Publications 213, 5-22.

Sparks S.R., Sigurdsson H., Wilson L., 1977. Magma mixing: a mechanism for triggering acid explosive eruptions. Nature 267(5609), 315-318.

Srivastava R.K. and Sinha A.K., 2004. Geochemistry and petrogenesis of early Cretaceous sub-alkaline mafic dykes from Swangkre-Rongmil, East Garo Hills, Shillong plateau, Northeast India. Journal of Earth System Science 113, 683-697.

Štemprok M., Dolejš D., Müller A., Seltmann R., 2008. Textural evidence of magma decompression, devolatilization and disequilibrium quenching: an example from the Western Krušné hory/Erzgebirge granite pluton. Contributions to Mineralogy and Petrology 155, 93-109.

Swanson S.E., 1977. Relation of nucleation and crystal-growth rate to the development of granitic textures. American Mineralogist 62, 966-978.

Tepley III F.J., Davidson J.P., Clynne M.A., 1999. Magmatic interactions as recorded in plagioclase phenocrysts of Chaos Crags, Lassen Volcanic Center, California. Journal of Petrology 40, 787-806.

Tischendorf G., Gottesmann B., Förster H.J., Trumbull R.B., 1997. On Li-bearing micas: estimating Li from electron microprobe analyses and an improved diagram for graphical representation. Mineralogical Magazine 61(409), 809-834.

Tuttle O.F. and Bowen N.L., 1958. Origin of granite in the light of experimental studies in the system NaAlSi3O8-KAlSi$_3$O$_8$-SiO$_2$-H$_2$O. The Geological Society of America 74, 1-153.

Underwood S.J., Feeley T.C., Clynne M.A., 2012. Hydrogen isotope investigation of amphibole and biotite phenocrysts in silicic magmas erupted at Lassen Volcanic Center, California. Journal of volcanology and geothermal research 227, 32-49.

Vernon R.H., 1983. Restite, xenoliths and microgranitoid enclaves in granites. Journal & Proceedings, Royal Society of New South Wales 116, 77-103.

Walker B.M., 1976. The origin of quartz-feldspar, graphic intergrowths. Ph.D. thesis, Michigan State University.

Wang W., Liu S., Bai X., Li Q., Yang P., Zhao Y., Guo R.,

2013. Geochemistry and zircon U-Pb-Hf isotopes of the late Paleoproterozoic Jianping diorite-monzonite-syenite suite of the North China Craton: implications for petrogenesis and geodynamic setting. Lithos 162, 175-194.

Whitney J.A., 1975. The effects of pressure, temperature, and X_{H2O} on phase assemblage in four synthetic rock compositions. The Journal of Geology 83, 1-31.

Woodruff D.P., 1973. The solid-liquid interface. Cambridge University Press Archive.

Lee J.I., 1997. A review on the origin of micrographic granites (Masanites) in the southern Kyongsang Basin, Korea. Geosciences Journal 1(4), 202-215.

Vernon R.H., 1990. Crystallization and hybridism in microgranitoid enclave magmas: microstructural evidence. Journal of Geophysical Research: Solid Earth 95(B11), 17849-17859.

Madelbrot B., 1967. How long is the cost of Britain? Statistical self-similarity and fractional dimension. Science 156, 636-638.

Hu X., Zhang B., Tang Q., Xu J., Fan D., Zhou W., 2018. Fractal analysis of amphibole aggregation growth from a basaltic melt and residual melt at high pressure and high temperature. Fractals 26(03), 1850032.

Huber M. and Stępniewska K., 2021. Application of the Fractal Dimension Calculation Technique to Determine the Shape of Selected Monchepluton Intrusion Crystals (NE Fennoscandia). Minerals 11, 1140.

Tammann G., 1925. The States of Aggregation Van Nostrand, New York.

Kirkpatrick R.J., 1975. Crystal growth from the melt: a review. American Mineralogist: Journal of Earth and Planetary Materials 60, 798-814.

Bouloton J. and Gasquet D., 1995. Melting and undercooled crystallisation of felsic xenoliths from minor intrusions (Jebilet massif, Morocco). Lithos 35(3-4), 201-219.

Winter J.D., 2001. An introduction to igneous and metamorphic petrology. Prentice-Hall, New Jersey.

Stewart D.B., 1959. Rapakivi granite from eastern Penobscot Bay, Maine. In 20th International Geological Congress, Mexico 293-320.